Plane Wave Imaging Using Phased Array

Arno Volker[a]

[a]*TNO, Stieltjesweg 1, P.O.box 155 2600 AD Delft, The Netherlands*

Abstract. Phased arrays are often used for rapid inspections. Phased arrays can be used to synthesize different wave fronts. For imaging, focused wave fronts are frequently used. In order to build an image, the phased array has to be fired multiple times at the same location. Alternatively, different data acquisition configurations can be designed in combination with an imaging algorithm. The objective of this paper is to use the minimal amount of data required to construct an image. If a plane wave is synthesized, the region of interest is illuminated completely. For plane wave synthesis, all elements in the phase array are fired. This ensures a good signal to noise ratio. Imaging can be performed efficiently with a mapping algorithm in the wavenumber domain. The algorithm involves only two Fourier transforms and can therefore be extremely fast. The obtained resolution is comparable to conventional imaging algorithms. This work investigates the potential and limitations of this mapping algorithm on simulated data. With this approach, frame rates of more than 1 kHz can be achieved

Keywords: Imaging, Phase Array, Ultrasonic Inspection
PACS: 43.35.Zc, 43.60.Fg, 81.70.Cv, 87.63.dh

INTRODUCTION

Phased arrays have become very common and real time imaging can be done with affordable hardware. More and more attention shifts towards full matrix capture, meaning that data is collected for all transmit-receive combinations in the array. With an increasing number of elements in the array, data acquisition times and processing times will start to increase. Particularly when going to full 2D arrays. Here we focus on an alternative method, which only requires one excitation of the array to completely image the sample. This in contrast to full matrix capture, which requires to fire N-times, where N equals the number of elements in the phased array.

We will demonstrate that illuminating the sample with a plane wave, which is the wave front that is generated when firing all elements simultaneously can provide a good image quality. Moreover it will be shown that the imaging itself can be performed very efficiently by double Fourier transform.

IMAGING BY FOURIER TRANSFORM

Imaging can be formulated in many different ways, frequently it is formulated as a summation over a travel time curve. The output of the summation forms one pixel in the image and this is repeated for all pixels. The travel time curve is either calculated by geometrical considerations or ray-tracing in case of more complicated media. Here we follow a slightly different approach, imaging is described by inverse wave field extrapolation and extracting the information at zero time. This information is transferred to the image.

In case of a plane wave excitation, the inverse wave field extrapolation involves subtracting the spatial phase due to the plane wave and the diffraction response of the medium. This is described mathematically by two complex exponentials:

$$p(x,y,\Delta z,t) = \int\int\int \tilde{P}\left(k_x,k_y,z=0,f\right) e^{jk\Delta z} e^{jk_z\Delta z} e^{-j\left(k_x x+k_y y-2\pi f t\right)} dk_x dk_y df, \quad (1)$$

Where $\tilde{\mathrm{P}}\left(\mathrm{k_x},\mathrm{k_y},\mathrm{z}=0,\mathrm{f}\right)$ is the recorded field by the phased array at $\mathrm{z}=0$, $\mathrm{k_x}$, $\mathrm{k_y}$ and $\mathrm{k_z}$ are the wavenumbers ($\mathrm{k}=\sqrt{\mathrm{k_x^2}+\mathrm{k_y^2}+\mathrm{k_z^2}}$) in the three different directions and f is the frequency. The wave field is extrapolated to a depth

40th Annual Review of Progress in Quantitative Nondestructive Evaluation
AIP Conf. Proc. 1581, 124-131 (2014); doi: 10.1063/1.4864811

Δz. If there is a diffractor/reflector at this depth, the information is at zero time. In order to obtain that information, we can write:

$$p(x, y, \Delta z, t = 0) = \int\int\int \tilde{P}\left(k_x, k_y, z = 0, f\right) e^{-j\left(k_x x + k_y y - k\Delta z - k_z \Delta z\right)} dk_x dk_y df. \quad (2)$$

If we now introduce the following coordinate transform

$$\mathrm{f} \rightarrow \mathrm{k}'_{\mathrm{z}} = \mathrm{k} + \mathrm{k}_{\mathrm{z}}, \quad (3)$$

the imaging of the data turns out to be an inverse Fourier transform:

$$\mathrm{p}(\mathrm{x}, \mathrm{y}, \Delta\mathrm{z}) = \int\int\int \frac{1}{\mathrm{J}} \tilde{\mathrm{P}}\left(\mathrm{k}_{\mathrm{x}}, \mathrm{k}_{\mathrm{y}}, \mathrm{z} = 0, \mathrm{f}\right) \mathrm{e}^{-\mathrm{j}\left(\mathrm{k}_{\mathrm{x}}\mathrm{x} + \mathrm{k}_{\mathrm{y}}\mathrm{y} - \mathrm{k}'_{\mathrm{z}}\Delta\mathrm{z}\right)} \mathrm{dk}_{\mathrm{x}} \mathrm{dk}_{\mathrm{y}} \mathrm{dk}'_{\mathrm{z}}, \quad (4)$$

where $\mathrm{J} = \frac{\partial \mathrm{k}'_{\mathrm{z}}}{\partial \mathrm{f}}$ is the jacobian of the coordinate transform, which is essentially an amplitude scaling of the data.

The means that the imaging can be expressed by the following steps:

- Fourier transform on input data in all directions;
- Interpolate data $\tilde{\mathrm{P}}\left(\mathrm{k}_{\mathrm{x}}, \mathrm{k}_{\mathrm{y}}, \mathrm{f}\right) \rightarrow \tilde{\mathrm{P}}\left(\mathrm{k}_{\mathrm{x}}, \mathrm{k}_{\mathrm{y}}, \mathrm{k}'_{\mathrm{z}}\right)$;
- Apply Jacobian;
- Inverse Fourier transform yields the image.

The scheme has been formulated in 3D $(\mathrm{x}, \mathrm{y}, \mathrm{z})$, but in case of 2D (x, z), the y and k_{y}variables can simply be dropped. The major advantage of the approach is that data acquisition can be performed extremely fast, but the imaging is also computationally very efficient allowing us to process large datasets in a very short amount of time. We will now illustrate the algorithm using a number of simple examples. As reference we use the pulse-echo image, meaning that each element of the phased array is fired separately and that the echo signals are recorded by the same element.

POINT DIFFRACTORS

We have modeled data for a 128 element phased array, with a center frequency of 4 MHz. A realistic bandwidth of 60% is used. The pitch of the element is 200 μm, which is state of the art for a composite piezo electric array. The height of the elements is 0.5 mm. The forward modeling is done using a semi-analytical code based on the Rayleigh II integral. This takes into account the directivity of each element. The forward modeling is done in the frequency domain, for all frequencies in the signal band. Two different dataset are modeled:

- Pulse-echo data;
- Plane wave excitation.

In case of pulse-echo data, each element in the array is fired separately and the back scattered signal is recorded on the same element. This requires obviously that 128 independent measurements have to be performed.

For plane wave imaging, all elements in the array are excited at the same time. This synthesizes a plane wave that illuminates the medium completely. The back scattered waves are recorded by all element. This provides a dataset that can be used for imaging.

Two different models (see Fig. 1) are used:

Case 1: horizontal array of point diffractors at 10 mm from the phase array;

Case 2: tilted array of point diffractors.

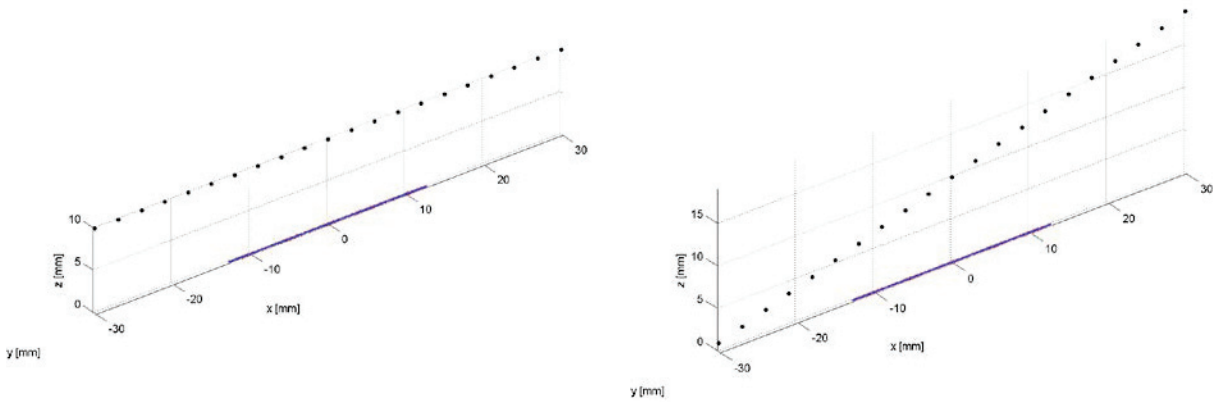

a) b)

FIGURE 1. Simulation geometries for the evaluation of the imaging algorithm, a) set of point diffractors parallel to array, b) tilting point diffractors to evaluate depth dependent resolution. The array is shown at z=0 and in the center of the x-axis.

The data generated for case 1 (horizontal array of diffractors) is shown in Fig. 2. Figure 2a shows the data for the pulse-echo case and Fig. 2b shows the data for the plane wave excitation. The apparent velocity is clearly different; the tail of the hyperbolic diffraction responses is twice as steep for the pulse-echo case compared to the plane wave data.

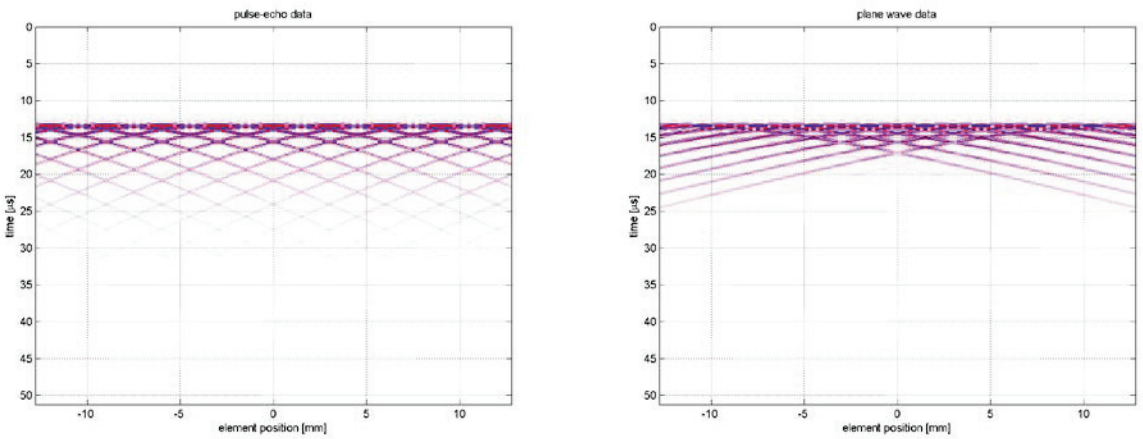

a) b)

FIGURE 2. Visualization of the modeled data, a) pulse-echo data, b) plane wave excitation data.

Both datasets are imaged, using similar algorithms. Dropping the plane wave term in equation (2) and taking the square of the wave field extrapolation operator [1] yields a similar algorithm for pulse-echo data. The results are shown in Fig. 3. The diffractors are numbered from 1 to 21 for convenience. Both datasets produce an image of the point diffractors. The pulse-echo data produces a slightly larger field of view, meaning that diffractors 6 and 16 are also imaged. Due to the plane wave excitation, only the diffractors below the aperture of the array are properly imaged. On the other hand the amount of noise is much less. The noise is caused by aliased signal.

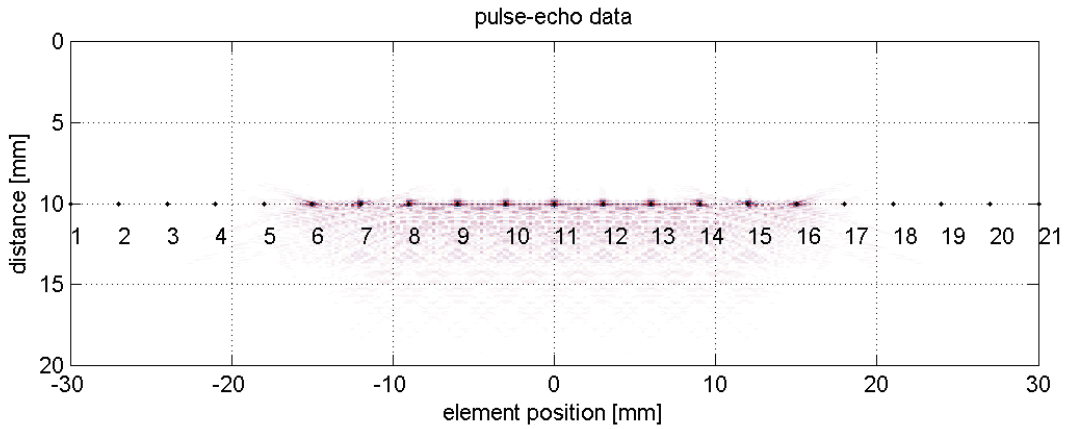

a)

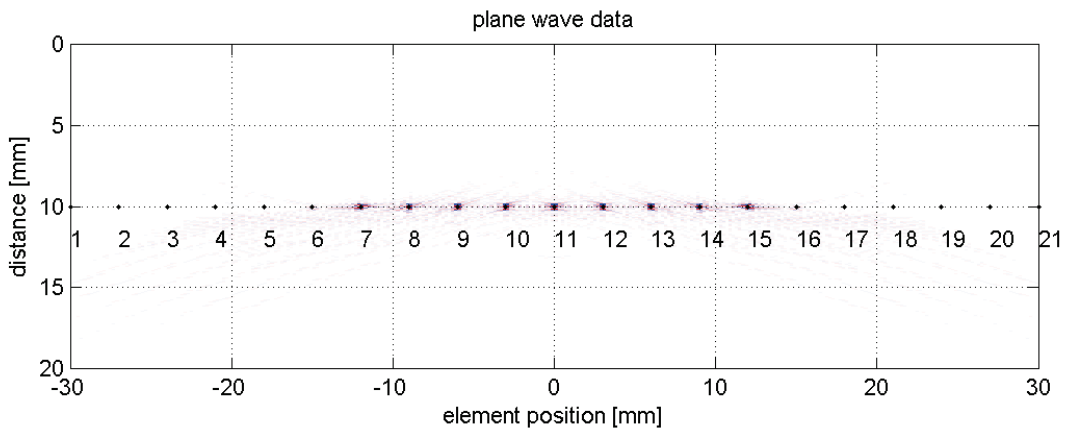

b)

FIGURE 3. Images obtained by applying the imaging algorithm, a) image of pulse echo data, b) image of plane wave excitation data. The point diffractors are also shown with an increasing number. The pulse-echo data provides a slightly large field of view, diffractors 6 and 16 are also imaged. The image for the plane wave excitation clearly contains less noise.

In order to compare the resolution, we calculated the maximum of the envelope of the images. The result is shown in Fig. 4. Again the higher noise in the pulse echo data is quite striking. Also the larger field of view of the pulse-echo data is clear because the amplitudes of the diffractor responses is more uniform. However the resolution is not very different, by looking at the width of the main lobe. This is surprising because the pulse-echo configuration is expected to provide a better resolution based on the steeper diffraction responses. However due to aliasing, the higher frequencies are not properly imaged. Low pass filtering of both datasets such that aliasing is minimized shows in fact a higher resolution for the pulse-echo dataset.

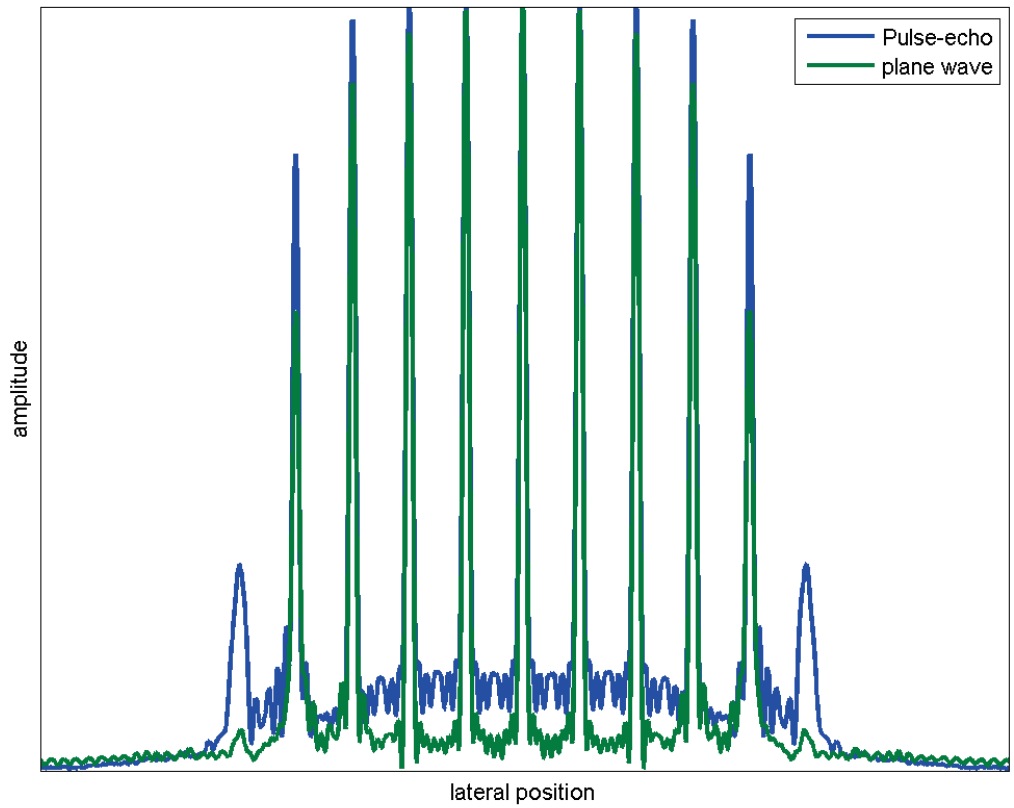

FIGURE 4. Point spread function for the pulse-echo and plane wave excitation, this indicates that for this geometry a similar resolution is obtained, but the plane wave image contains much less aliasing noise. The field of view, i.e., the diffractor amplitude as function of the lateral position is larger for the pulse-echo acquisition configuration.

In order to assess the image quality as function of depth, a slanted array of point diffractors is modeled. The images obtained for both datasets are shown in Fig. 5. Again we see much more noise for the pulse-echo data, particularly at more shallow depths. Obviously there is more serious aliasing in this case due to the larger angle range at which the scattered waves arrive at the array.

For the plane wave data, the shallow diffractors responses near the end of the array show some ‘smiles’, due to aperture limitations. In this case, only half sided hyperbolic diffraction curves are recorded, causing these artifacts. The same type of artifacts is present in the image from the pulse-echo data, but these are masked by the aliasing noise to a large extent. Again much less aliasing noise is observed and the resolution is quite similar.

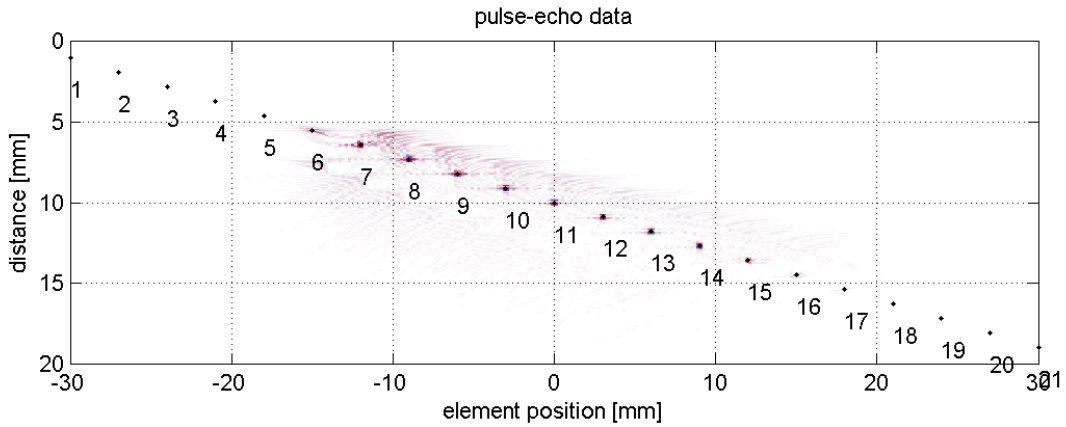

a)

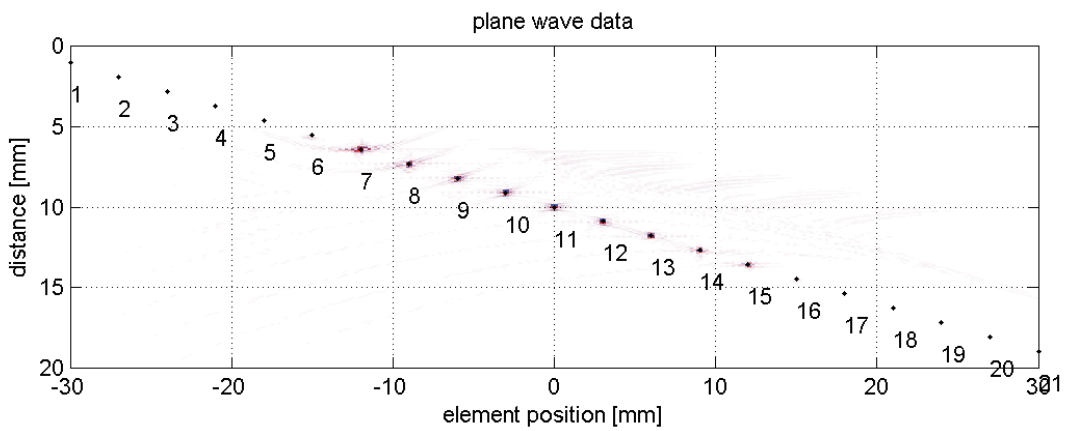

b)

FIGURE 5. Image of tilting set of point diffractors, a) image of pulse echo data, b) image of plane wave excitation data. The point diffractors are also shown with an increasing number. The pulse-echo data provides a slightly larger field of view: diffractors 6 and 16 are also imaged. The image for the plane wave excitation clearly contains less noise.

PLANAR DEFECTS

Apart from point diffractors we evaluate the response from planar defects. In this case the defect causes some directivity and the main question is up to what angle will these defects be properly imaged? The tilt angle of the defects is varied from 0 to 60°. The length of each defect is 2 mm. Figure 6 shows the images for both acquisitions. Again we observed that the pulse-echo data is capable of imaging steeper defects, the defect at 30° is still imaged for the pulse-echo data. For the plane wave data, only the diffractions from the edges are imaged. If it is known that defects are predominantly at one specific angle, it is possible to generate planes waves for that angle, which will improve the image.

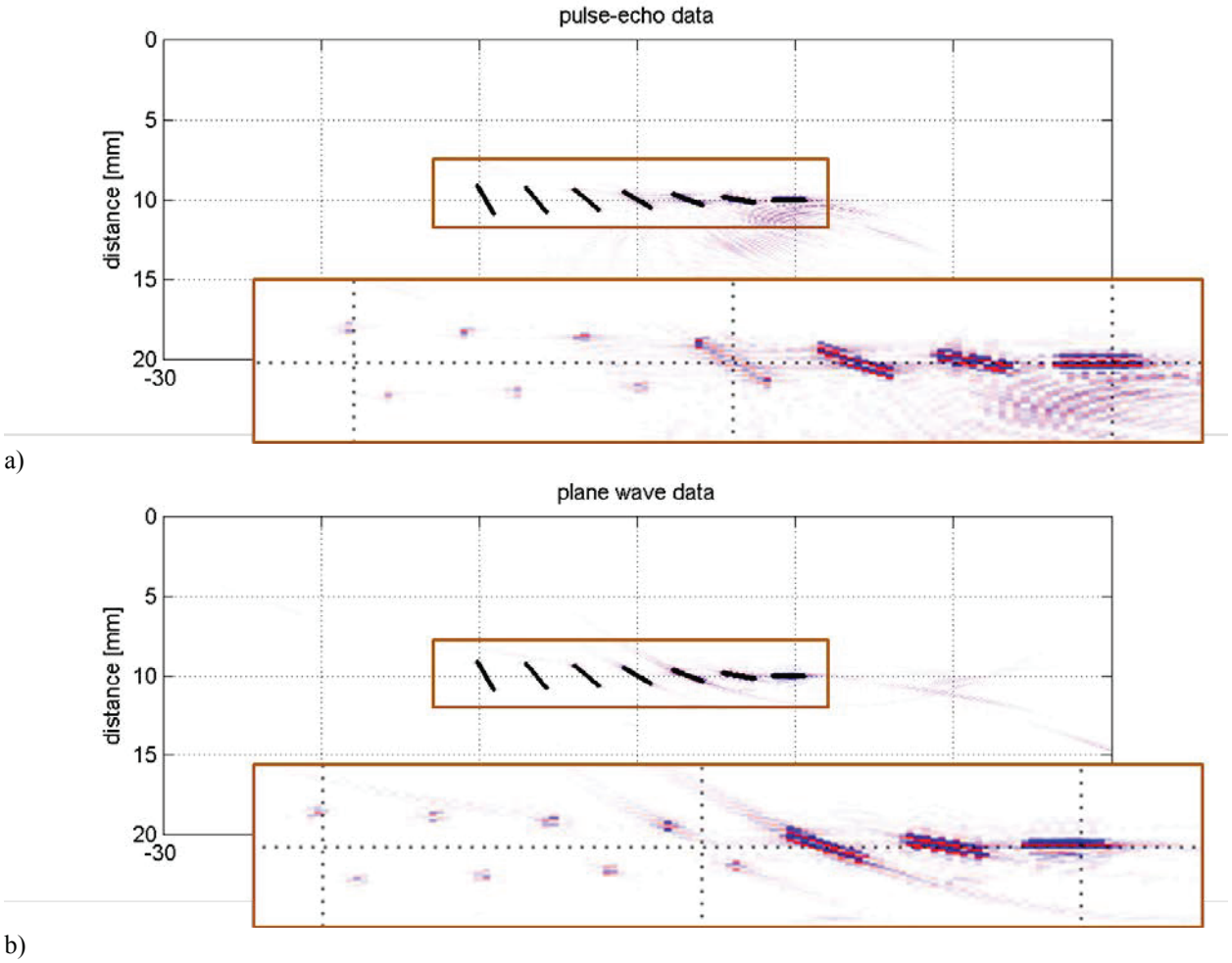

FIGURE 6. Image of spatially extended defects, a) image of pulse echo data, b) image of plane wave excitation data. The pulse-echo data provides a slightly large tilt angle range in which the complete defect is imaged, the edge diffractions are always imaged and can be used for accurate sizing.

CONCLUDING REMARKS

We have demonstrated that plane wave can efficiently be used for very rapid imaging. By illuminating a sample with a plane wave, it is possible to collect a dataset which provides high quality images. This allows an extremely high frame rate, which is particularly useful for rapid moving media.

It has been shown that it is possible to image the data using a very efficient mapping in the wave number domain. This imaging algorithm essentially consists of a Fourier transform, interpolation and amplitude scaling and then an inverse Fourier transform.

An additional advantage is that in case of plane waves, sampling requirement are much less stringent as for example in case of pulse-echo data. Therefore a similar resolution can be achieved, with less artifacts. This helps to obtain a large field of view, due to the use of a larger pitch of the elements in the phased array. The field of view for pulse-echo data is in fact slightly larger than using a plane wave excitation, but obviously the acquisition time is substantially longer.

REFERENCES

1. R. H. Stolt, *Migration by Fourier Transform*, Geophysics, Vol. 43, No 1, February 1978.